Ocean Systems Engineering, *Vol. 5, No. 3 (2015) 181-198*
DOI: http://dx.doi.org/10.12989/ose.2015.5.3.181

Lifting off simulation of an offshore supply vessel considering ocean environmental loads and lifting off velocity

Dong-Hoon Jeong[1a], Myung-Il Roh[*2] and Seung-Ho Ham[1b]

[1]*Department of Naval Architecture and Ocean Engineering, Seoul National University, 1 Gwanak-ro, Gwanak-gu, Seoul, 08826, Republic of Korea*
[2]*Department of the Naval Architecture and Ocean Engineering, and Research Institute of Marine Systems Engineering, Seoul National University, 1 Gwanak-ro, Gwanak-gu, Seoul, 08826, Republic of Korea*

(Received July 8, 2015, Revised August 15, 2015, Accepted September 1, 2015)

Abstract. An OSV (Offshore Support Vessel) is being used to install a structure which is laid on its deck or an adjacent transport barge by lifting off the structure with its own crane, lifting in the air, crossing splash zone, deeply submerging, and lastly landing it. There are some major considerations during these operations. Especially, when lifting off the structure, if operating conditions such as ocean environmental loads and lifting off velocity are not suitable, the collision can be occurred due to the relative motion between the structure and the OSV or the transport barge. To solve this problem, this study performs the physics-based simulation of the lifting off step while the OSV installs the structure. The simulation includes the calculation of dynamic responses of the OSV and the structure, including the collision detection between the transport barge and the structure. To check the applicability of the physics-based simulation, it is applied to a problem of the lifting off step by varying the ocean environmental loads and the lifting off velocity. As a result, it is confirmed that the operability of the lifting off step are affected by the conditions.

Keywords: offshore support vessel; lifting off; physics-based simulation; ocean environmental loads; lifting off velocity

1. Introduction

1.1 Research background

1.1.1 Offshore installation methods

The particular characteristics of an offshore structure are not like those of an onshore or near-shore structure. Thus, it cannot be constructed in its actual site, and might be built in shipyard, transferred, transported to the site, and finally deployed at there. There are various methods to transfer, transport, and deploy it, as shown in Fig. 1.

The transferring operation is that an offshore structure is moved from shipyard to means of transporting. The major methods of the transferring operation are a loading out method, a floating

∗Corresponding author, Associate professor, E-mail: miroh@snu.ac.kr
[a] Graduate student, E-mail: jdh0111@snu.ac.kr
[b] Graduate student, E-mail: hsh0930@snu.ac.kr

http://www.techno-press.org/?journal=ose&subpage=7 ISSN: 2093-6702 (Print), 2093-677X (Online)

out method, and a lifting off method. The loading out method is carried out by moving the offshore structure onto a transport barge in the longitudinal or transverse direction of the barge. And, in the case of the floating out method, the offshore structure such as a jacket substructure and a load tower fabricated in a dry dock is brought afloat and floated out from the fabrication site like the launching of a ship. Lastly, the lifting off method is that an offshore structure such as an offshore module and a deck structure is lifted off and moved by the crane of an OSV (Offshore Support Vessel).

The offshore structure moved to the means of transporting can be transported to its actual site by some methods such as a barge towing method, a self-floating towing method, and a self-propelled carrier transporting method. The barge towing method is to transport the offshore structure resting on a transport barge by several tugs. In the case of the self-floating towing method, the offshore structure is supported by not a transport barge but its own buoyancy and pushed or pulled by tugs. And, the self-propelled carrier transporting method is that a transport barge or an OSV transports the offshore structure resting on the deck by its own propulsion.

Finally, the offshore structure arrives at the site. Then, by some methods such as a floating over method, a launching method, and a lifting method, the offshore structure can be deployed. Both the launching method and the floating over method take advantage of ballasting of a transport barge when loading the offshore structure. However, the launching method obtains the slope of the transport barge by ballasting and pulls the offshore structure forward while the float over method mates the offshore structure onto the fixed structure by changing the draft of the transport barge. In the case of the lifting method, the offshore structure is lifted and moved by the crane of the OSV.

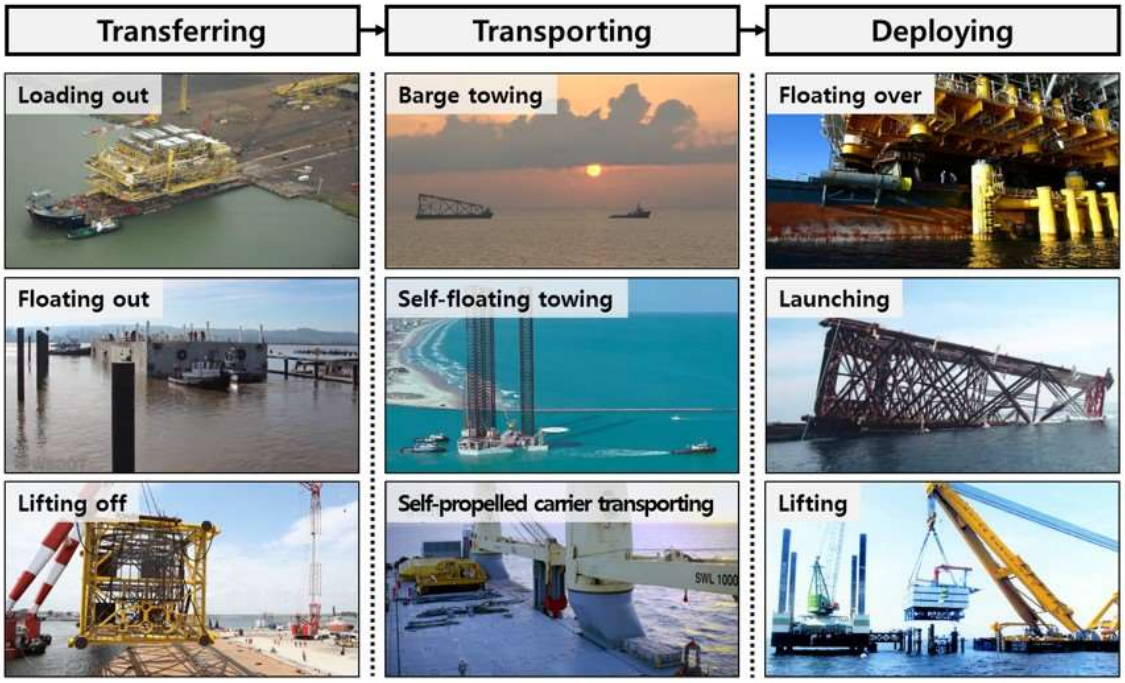

Fig. 1 Overview of offshore installation methods

These methods for transferring, transporting, and deploying operations are selected depending on some considerations such as the circumstances or characteristics of the offshore structure. Also, each method has its own considerations during the operation. Among them, considerations of the lifting method for the deploying operation are described in the next section.

1.1.2 Lifting method for deploying operation

An offshore structure is transported to the actual site after constructed on shore. The transported offshore structure is deployed in the way of something such as float-over, launching, and lifting. Among them, the lifting method is usually carried out by an OSV and it consists of five steps (Nielsen 2003), as shown in Fig. 2.

There are some major considerations on each step in the lifting method. In the 'lifting off' step (Fig. 2(a)), an OSV lifts off the offshore structure which is laid on the deck or the adjacent transport barge with its own crane. At this moment, there should be no collision between the offshore structure and others resulting from the relative motion among them. In the 'lifting in the air' step (Fig. 2(b)), the lifted offshore structure is moved to the specified site in the air. In this process, the significant and undesirable pendulum motion should be avoided because it is very important to control the offshore structure exactly. The offshore structure penetrates the water surface in the 'crossing splash zone' step (Fig. 2(c)). The varying buoyancy force and slamming impact force exerted on the offshore structure should be considered in this step. In the 'deeply submerging' step (Fig. 2(d)) in which the offshore structure is submerged deeply, the motion of the lifted offshore structure, in response to wave induced motion of the OSV crane tip, is important because of the possibility of resonance. In the last 'landing' step (Fig. 2(e)), one should land the offshore structure exactly and there should not be large impact which could cause damage to the offshore structure.

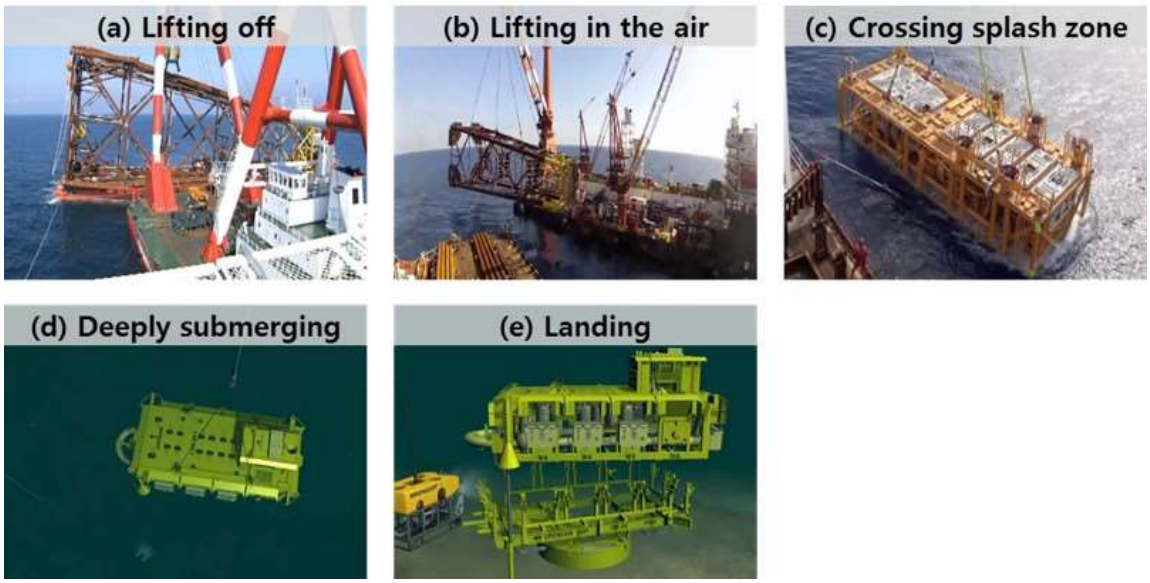

Fig. 2 Five steps of the lifting method by the OSV

If we can simulate each step in the aspect of the above major considerations, we are able to verify the validity of operation conditions. Thus, physics-based simulation based on multibody system dynamics is performed for the lifting off step. Through the simulation, the tension acting on wire ropes of the OSV crane and collision between the transport barge and the offshore structure are analyzed. At this time, various operating conditions such as ocean environmental loads and lifting off velocity are applied to the simulation.

1.2 Related studies

There are some studies related to the simulation in the field of ship production. Cha *et al.* (2010a) proposed an integrated simulation framework for shipbuilding production. The proposed simulation framework provides an environment for developing various simulation systems for shipbuilding process planning. It consists of a simulation kernel, basic simulation component and application-specific simulation component. Cha *et al.* (2010b) performed dynamic response simulation of a heavy cargo suspended by a floating crane. The dynamic equations of motions of the floating crane and the heavy cargo were considered by coupled equations because the floating crane and the heavy cargo are connected by wire ropes and provide a force and a moment for each other. Also, the nonlinear hydrostatic force, the linear hydrodynamic force, the wire rope force, and the mooring force were considered as external forces. And, they estimated the motion of the floating crane and the heavy cargo, and also calculated the tension acting on the wire ropes between the two. Ha *et al*. (2015) developed a multibody system dynamics simulator for the process simulation of ships and offshore structures. The developed simulator consists of six components: the multibody system dynamics kernel, the force calculation kernel, the numerical analysis kernel, the hybrid simulation kernel, the scenario management kernel, and the collision detection kernel. They applied the simulator to various cases of the process simulation of the ships and the offshore structures.

There are also some studies related to the simulation in the field of offshore engineering, especially the lifting method for deploying operation. Masoud (2000) applied delayed-position feedback together with luff-and-slew angle actuation to a vessel crane in order to control pendulum motion of a lifted structure in the air.

Table 1 Summary of related studies and comparison with this study

Studies	Applying step	Purpose	Wire tension	Collision	Ocean environmental loads	Lifting off velocity
Masoud (2000)	Lifting in the air	Method of minimizing pendulum motion of lifted load	X	X	X	X
Wu (2013)	Crossing splash zone	Dynamic response of the template through splash zone	O	X	O	X
Boe and Nestegard (2010)	Deeply submerging	The development of the dynamic response equation	O	X	O	X
This study	Lifting off	Analysis of wire tension and collision	O	O	O	O

And, the effectiveness of this method was demonstrated with a fully nonlinear three-dimensional computer simulation and with an experiment on a 1/24 scale model. Wu (2013) analyzed dynamic response of a template suspended by a floating crane through splash zone. Wu carried out dynamic and static analysis by using the SIMA (Simulation workbench for Marine Applications). Boe and Nestegard (2010) developed dynamic response equations of the lifted structure in deep water and described how these equations can be applied in order to establish limiting sea-states for the operation.

As shown in Table 1, the studies mentioned above did not cover dynamic responses such as wire tension and collision, and various operating conditions such as ocean environmental loads and lifting off velocity all in the lifting off step. Thus, this study performs the physics-based simulation of the lifting off step while the OSV installs the structure. The simulation includes the calculation of the dynamic responses of the OSV and the structure, including the collision detection between the transport barge and the structure.

2. Theoretical backgrounds of lifting off simulation

Fundamentally, the Newton's 2nd law might be applied to describe the motion of the OSV, the transport barge, and the offshore structure. Thus, it can be said that this simulation is based on physics. For this physics-based simulation to be acknowledged and elaborated, multibody system dynamics, hydrodynamics force, wire tension, and collision process are required additionally.

2.1 Multibody system dynamics

A vessel-mounted crane can be regarded as a multibody system which consists of interconnected rigid bodies. Thus, the equations of motion based on multibody system dynamics is required to analyze the motion of an object including crane system. In this section, the equations of motion based on the multibody system dynamics is explained (Shabana 1994).

The relative motion that is permitted between bodies in the multibody system is often constrained by connections between those bodies. Therefore, Newton's equation of motion for the multibody system is

$$\mathbf{M}\ddot{\mathbf{r}} = \mathbf{F}^{\mathbf{e}} + \mathbf{F}^{\mathbf{c}} \tag{1}$$

The vectors in Eq. (1) are represented in terms of the Cartesian coordinates. **M** is the mass and the mass moment of inertia matrices and **r** is the position vector of the center of gravity of the bodies with respect to the Cartesian coordinates. The resultant force is composed of the external force $\mathbf{F}^{\mathbf{e}}$ and the constraint force $\mathbf{F}^{\mathbf{c}}$ caused by kinematic constraints.

The position vector **r** of the Cartesian coordinates can be presented as a function of the generalized coordinates **q** according to

$$\mathbf{r} = \mathbf{r}(\mathbf{q}) \tag{2}$$

Differentiating Eq. (2) yields the velocity relation

$$\dot{\mathbf{r}} = \mathbf{J}\dot{\mathbf{q}} \tag{3}$$

where, the velocity transformation matrix **J** transforms the velocity of generalized coordinates $\dot{\mathbf{q}}$

into the velocity of the Cartesian coordinates.

Differentiating Eq. (3) yields the acceleration

$$\ddot{\mathbf{r}} = \mathbf{J}\ddot{\mathbf{q}} + \dot{\mathbf{J}}\dot{\mathbf{q}} \tag{4}$$

Substituting Eq. (4) into Eq. (1), we obtain the equation

$$\mathbf{M}\mathbf{J}\ddot{\mathbf{q}} + \mathbf{M}\dot{\mathbf{J}}\dot{\mathbf{q}} = \mathbf{F}^{\mathbf{e}} + \mathbf{F}^{\mathbf{c}} \tag{5}$$

Multiplying both sides of Eq. (5) by $\mathbf{J}^{\mathbf{T}}$ yields

$$\mathbf{J}^{\mathbf{T}}\mathbf{M}\mathbf{J}\ddot{\mathbf{q}} + \mathbf{J}^{\mathbf{T}}\mathbf{M}\dot{\mathbf{J}}\dot{\mathbf{q}} = \mathbf{J}^{\mathbf{T}}\mathbf{F}^{\mathbf{e}} + \mathbf{J}^{\mathbf{T}}\mathbf{F}^{\mathbf{c}} \tag{6}$$

The constraint reaction forces are perpendicular to the path along which the bodies are constrained to move. This suggests that the constraint reaction force $\mathbf{F}^{\mathbf{c}}$ may be suppressed by taking the scalar product of both sides of Newton's equation of motion with vectors that are tangent to the path. Then, we can derive

$$\tilde{\mathbf{M}}\ddot{\mathbf{q}} + \tilde{\mathbf{k}} = \tilde{\mathbf{F}}^{\mathbf{e}} \tag{7}$$

where $\tilde{\mathbf{M}} = \mathbf{J}^{\mathbf{T}}\mathbf{M}\mathbf{J}$, $\tilde{\mathbf{k}} = \mathbf{J}^{\mathbf{T}}\mathbf{M}\dot{\mathbf{J}}\dot{\mathbf{q}}$, and $\tilde{\mathbf{F}}^{\mathbf{e}} = \mathbf{J}^{\mathbf{T}}\mathbf{F}^{\mathbf{e}}$; $\tilde{\mathbf{M}}$ is the mass and the generalized mass moment of the inertia matrix, $\tilde{\mathbf{k}}$ is the generalized Coriolis and centrifugal force, $\tilde{\mathbf{F}}^{\mathbf{e}}$ is the generalized external force, $\mathbf{J}$ is the velocity transformation matrix, $\dot{\mathbf{J}}$ is the acceleration transformation matrix and $\mathbf{q}$ is the generalized coordinate of the multibody system. Eq. (7) is the final form of the equation of motion based on multibody system dynamics.

2.2 Hydrodynamic force calculation

Lifting operation is carried out offshore. Thus, hydrodynamic force would be exerted on an OSV or a transport barge and should be added to external forces of the equations of motion based on the multibody system dynamics. The hydrodynamic force can be divided into two parts, as shown in Eq. (8); the wave exciting force exerted by the incident wave and the diffraction wave, and the radiation force from the wave generated by the motion of the OSV itself.

$$\mathbf{F}_{Hydrodynamic} = \mathbf{F}_{Exciting} + \mathbf{F}_{Radiation} \tag{8}$$

$\mathbf{F}_{Exciting}$ can be calculated by the force RAO (Response Amplitude Operator) times the sinusoidal function at a given frequency. The force RAO can be obtained from a commercial solver. Cummins equation (Cummins 1962) can be used to calculate $\mathbf{F}_{Radiation}$ in the time domain. The added mass $a_{ij}(\omega)$ and the damping coefficient $b_{ij}(\omega)$ can also be obtained from the commercial solver. Fig. 3 summarizes the calculation procedure.

2.3 Wire tension calculation

An offshore structure is lifted by a vessel-mounted crane and the offshore structure and the crane are connected by wire ropes. When the offshore structure is lifted, these wire ropes are extended and exert tension. On the other hand, when these wire ropes are not extended, they are

loosened and exert no force. Thus, they could be modeled as incompressible springs which exert force only when extended. And, the force by the incompressible springs is added to external forces of the equations of motion based on the multibody system dynamics. The modeling of the incompressible spring force is presented in Fig. 4.

2.4 Collision process

Collision is the major consideration in the lifting operation, especially in the lifting off step. This study introduces collision process through changing the velocity (Moore and Wilhelms 1988, Chris 1997) to the physics-based simulation in order to consider collision between objects. In this section, the collision process in the case of 2D collision is explained, as shown in Fig. 5.

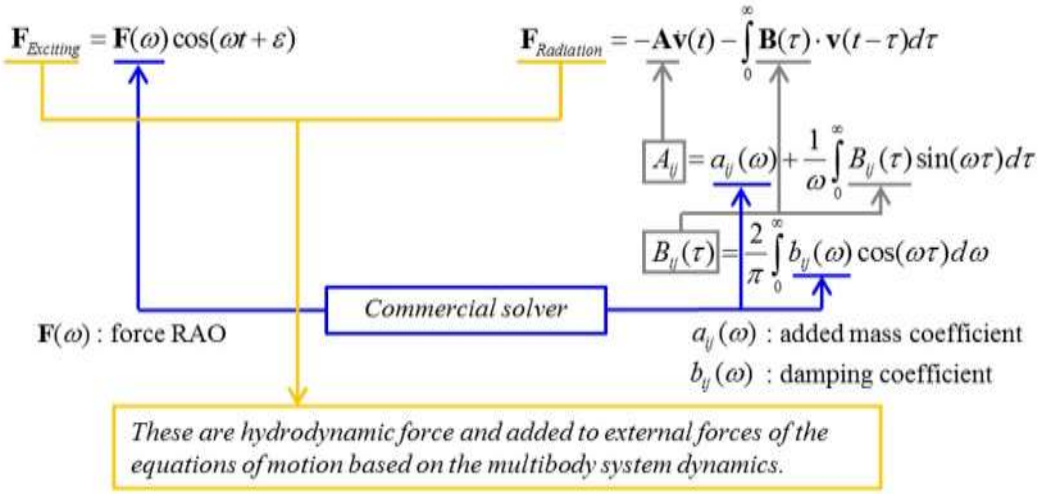

Fig. 3 Calculation procedure of the hydrodynamic force

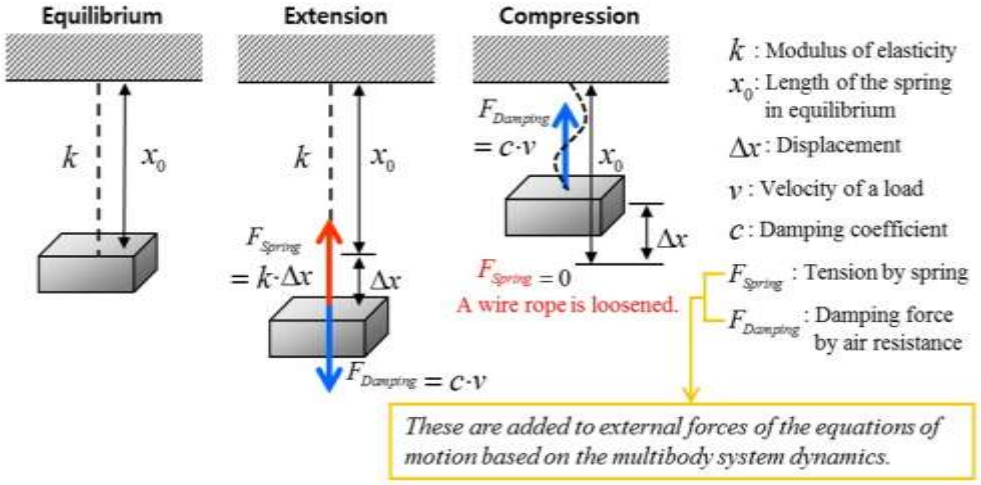

Fig. 4 Modeling of the incompressible spring force

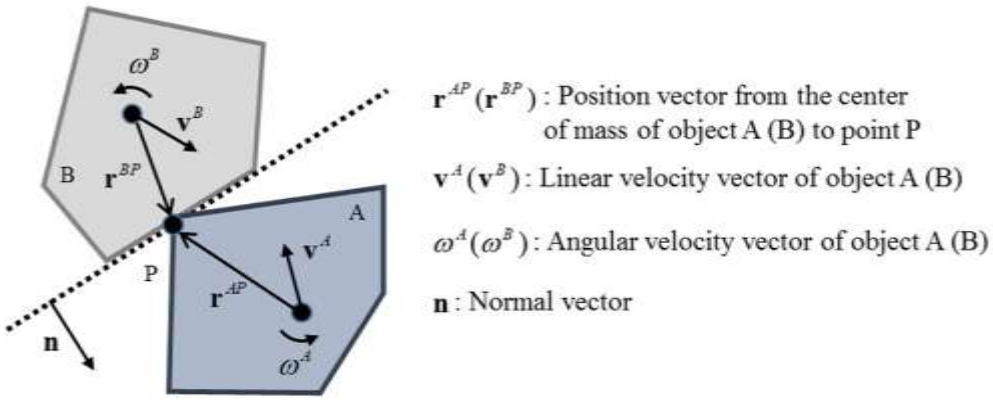

Fig. 5 Configuration of the objects A and B colliding each other

The collision process handles collision by changing the velocity of the objects which collide before and after collision. First, to check whether some objects collide or not, the penetration depth is defined. The penetration depth means how much the objects which collide penetrate each other before collision process. The step to determine the penetration depth is 'Collision detection'. Also, in this step, the normal vector (**n**) is obtained and necessary for the next step 'Collision response' in which the velocity of the objects is changed if they collide.

In the 'Collision response' step, the linear velocity and angular velocity are changed by following Eqs. (9) and (10).

$$\mathbf{v}_2^A = \mathbf{v}_1^A + \frac{i}{M^A}\mathbf{n} \tag{9}$$

$$\omega_2{}^A = \omega_1{}^A + \frac{\mathbf{r}^{AP} \cdot i\mathbf{n}}{I^A} \tag{10}$$

where subscripts 1 and 2 mean before and after collision, respectively. M^A means the mass of the object A, I^A means the moment of inertia of the object A, i means the magnitude of impulse by collision, '$\cdot$' operator means perp-dot product which means the magnitude of cross products of two vectors.

Eqs. (9) and (10) show how the collision affects pre-collision velocity of the object A. The equations for the object B are the same when i is replaced with $-i$. These equations can be obtained from Newton's law of motion. According to Newton's law of motion, the impulse is same with the change of momentum as following Eq. (11).

$$\mathbf{I} = M^A(\mathbf{v}^A{}_2 - \mathbf{v}^A{}_1) \tag{11}$$

where **I** means impulse.

Dividing both sides of Eq. (11) by M^A yields

$$\frac{\mathbf{I}}{M^A} = \mathbf{v}^A{}_2 - \mathbf{v}^A{}_1 \tag{12}$$

The direction of **I** is same with the direction of **n** and thus **I** can be expressed as the product of i and **n** as presented in Eq. (13).

$$\frac{i\mathbf{n}}{M^A} = \mathbf{v}^A{}_2 - \mathbf{v}^A{}_1 \tag{13}$$

Transposing $\mathbf{v}^A{}_1$ in Eq. (13) yields Eq. (9). Eq. (10) can be obtained in the same way for angular impulse and momentum.

Now, we should know how to calculate i to use Eqs. (9) and (10). i can be obtained from Newton's law of restitution. Newton's law of restitution can be expressed as Eq. (14)

$$\mathbf{v}^B{}_2 - \mathbf{v}^A{}_2 = -e(\mathbf{v}^B{}_1 - \mathbf{v}^A{}_1) \tag{14}$$

where e means coefficient of restitution.

And, Eq. (14) can be expressed as Eq. (15) by substituting $\mathbf{v}^B - \mathbf{v}^A$ to $\mathbf{v}^{AP} - \mathbf{v}^{BP}$ and perp-dot product of **n**.

$$(\mathbf{v}^{AP}{}_2 - \mathbf{v}^{BP}{}_2)\cdot\mathbf{n} = -e(\mathbf{v}^{AP}{}_1 - \mathbf{v}^{BP}{}_1)\cdot\mathbf{n} \tag{15}$$

where $\mathbf{v}^{AP}(\mathbf{v}^{BP})$ is the velocity vector of point P relative to the center of mass of the object A (B) and can be presented as Eq. (16).

$$\mathbf{v}^{AP}{}_2 = \mathbf{v}^A{}_2 + \omega^A{}_2\mathbf{r}^{AP} \tag{16}$$

Substituting Eqs. (9) and (10) to Eq. (16) yields

$$\mathbf{v}^{AP}{}_2 = \mathbf{v}^A{}_1 + \frac{i}{M^A}\mathbf{n} + (\omega^A{}_1 + \frac{\mathbf{r}^{AP}\cdot i\mathbf{n}}{I^A})\mathbf{r}^{AP} \tag{17}$$

By doing so for object B, Eq. (18) can be derived.

$$\mathbf{v}^{BP}{}_2 = \mathbf{v}^B{}_1 - \frac{i}{M^A}\mathbf{n} + (\omega^B{}_1 - \frac{\mathbf{r}^{BP}\cdot i\mathbf{n}}{I^A})\mathbf{r}^{BP} \tag{18}$$

Substituting Eqs. (17) and (18) to Eq. (15) and transposing terms out about i yields

$$i = \frac{-(1+e)\mathbf{v}^{AB}{}_1\cdot\mathbf{n}}{\mathbf{n}\cdot\mathbf{n}(\frac{1}{M^A}+\frac{1}{M^B}) + \frac{(\mathbf{r}^{AP}\cdot\mathbf{n})^2}{I^A} + \frac{(\mathbf{r}^{BP}\cdot\mathbf{n})^2}{I^B}} \tag{19}$$

Finally, i can be obtained from Eq. (19). And, we can process collision by using Eqs. (9) and (10).

The simple example for the validation of this collision process is presented in Fig. 6. Fig. 6(b) shows the graph of the bounced height of the ball according to variation of the coefficient of restitution.

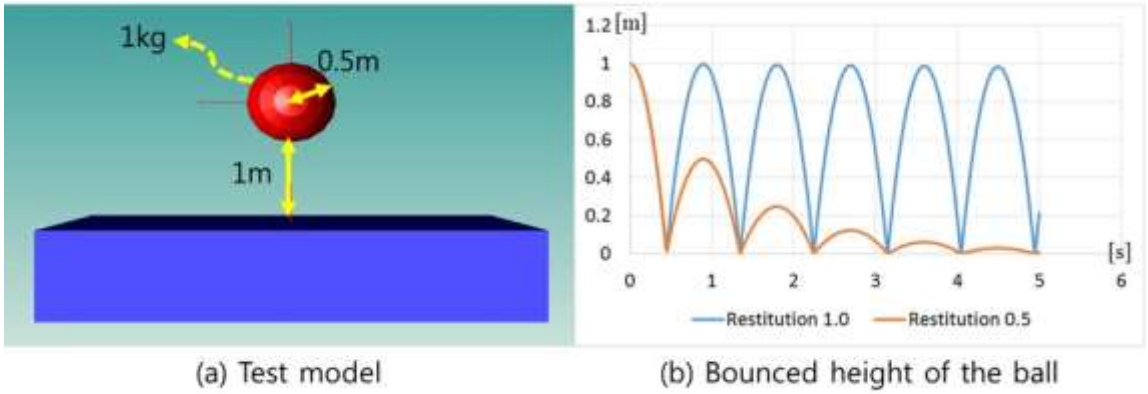

Fig. 6 Example for the validation of collision process

3. Lifting off simulation of the offshore supply vessel

3.1 Problem definition

Numerical model based on multibody system dynamics was validated through various examples in our previous studies (Ku *et al.* 2013a, 2013b, 2014). Similar to these examples, this study simulated the lifting off step of an OSV as shown in Fig. 7. Through this simulation, wire tension and collision during the lifting off step were analyzed. This simulation was carried out in various ocean environmental loads and lifting off velocity. The ocean environmental loads are affected by heading angle, wave height, and wave period. The directions of the heading angle are presented in Fig. 8. To prevent the state of trim by stem of the OSV to be generated during operation, the state of trim by stern was set to 1˚ as an initial condition. Fig. 8 and Table 2 is about the specification of these models in Fig. 7(b).

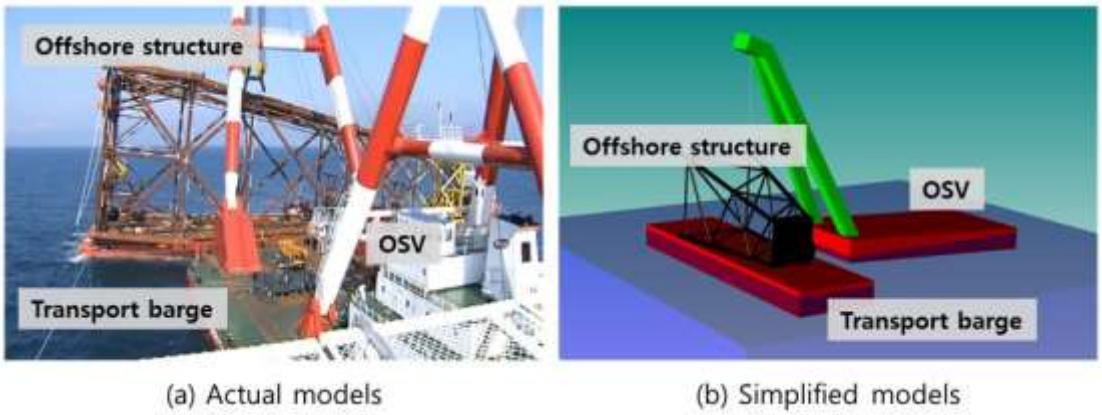

Fig. 7 Actual and simplified models for the lifting off simulation

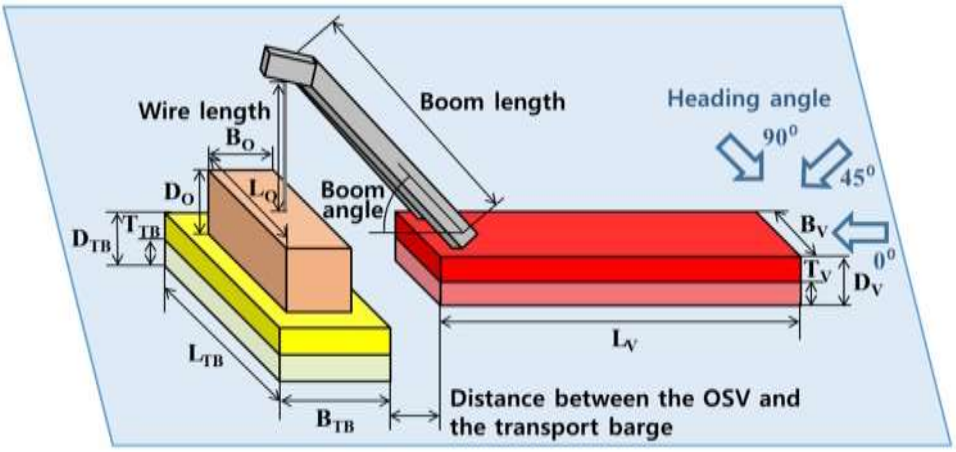

Fig. 8 Configuration of the simplified models for the lifting off simulation

Table 2 Specification of the OSV, the transport barge, and the offshore structure for the lifting off simulation

OSV			
Length (L_V) [m]	83	Boom length [m]	86
Breadth (B_V) [m]	44	Boom angle [deg]	60
Depth (D_V) [m]	6.4	Modulus of elasticity [kN/m]	10^4
Draft (T_V) [m]	4	Wire length [m]	37.6
Displacement [ton]	14,973	Capacity [ton]	1,800
Transport barge			
Length (L_{TB}) [m]	122.45	Draft (T_{TB}) [m]	6
Breadth (B_{TB}) [m]	30.5	Displacement [ton]	21,969
Depth (D_{TB}) [m]	7.6	Distance between the OSV and the transport barge	23.25
Offshore structure			
Length (L_O) [m]	70	Depth (D_O) [m]	20
Breadth (B_O) [m]	20	Weight (Mass) [ton]	1,000

3.2 Case studies

3.2.1 Variation of wave height

Table 3 shows simulation results in which the wave height is varying from 0.2 m to 0.8 m, the wave period is 11.4 s, the heading angle is 45˚, and the lifting off velocity is 0.1 m/s. In this table, a dynamic amplitude factor means a value of maximum dynamic load divided by static load. This static load means the weight of the offshore structure in the air. If there is no collision, it is 'X' and otherwise, it is 'O'. As shown in this table, there was no collision when the wave height is 0.2 m and 0.4 m but there was collision when the wave height is 0.6 m and 0.8 m. The dynamic amplitude factor was the highest in Case 4. Fig. 9 shows the simulation results of Case 4. Fig. 9(a) shows the change of wire tension as time goes and Fig. 9(b) shows the moment of collision between the transport barge and the offshore structure.

Table 3 Simulation results according to the variation of wave height

Case	Wave height [m]	Wave period [s]	Heading angle [deg]	Lifting off velocity [m/s]	Maximum wire tension [ton]	Dynamic amplitude factor	Collision
1	0.2	11.4	45	0.1	1,040.944	1.041	X
2	0.4				1,066.112	1.066	X
3	0.6				1,081.989	1.082	O
4	0.8				1,128.982	**1.129**	O

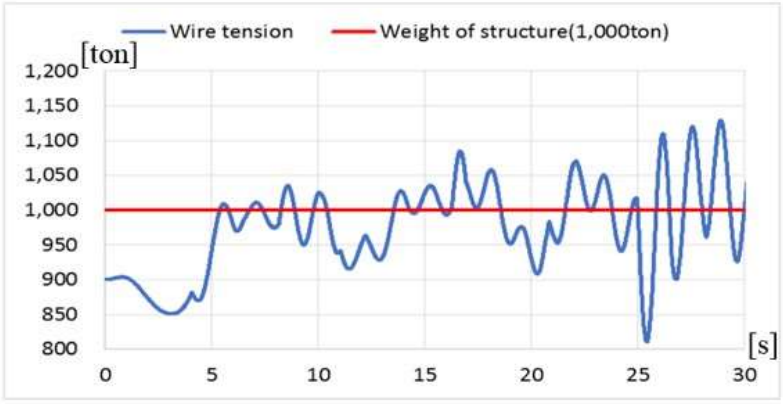

(a) Wire tension

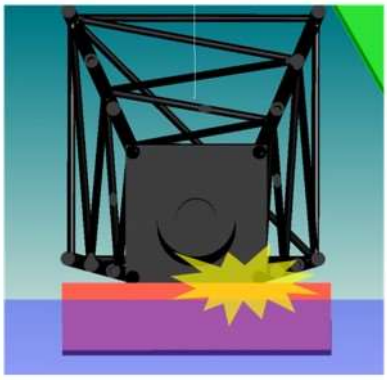

(b) Collision

Fig. 9 Simulation results of Case 4

3.2.2 Variation of heading angle

Table 4 shows simulation results in which the wave height is 0.4 m and 0.6 m, the wave period is 11.4 s, the heading angle is varying from 45˚ to 90˚, and the lifting off velocity is 0.1 m/s. Regardless of the wave height of 0.4 m or 0.6 m, there was no collision when the heading angle is 0˚ but there was collision when the heading angle is 90˚. On the other hand, according to the wave height of 0.4 m or 0.6 m, the occurrence of collision was different when the heading angle 45˚. The dynamic amplitude factor was the highest in Case 10. Fig. 10 shows the simulation results of Case 10. Fig. 10(a) shows the change of wire tension as time goes and Fig. 10(b) shows the moment of collision.

3.2.3 Variation of lifting off velocity

Table 5 shows simulation results in which the wave height is 0.2 m, the wave period is 11.4 s, the heading angle is 45˚, and the lifting off velocity is varying from 0.04 m/s to 0.07 m/s. There was no collision when the lifting off velocity is 0.06 m/s and 0.07 m/s but there was collision when the lifting off velocity is 0.04 m/s and 0.05 m/s. The dynamic amplitude factor was the highest in Case 14. In the cases of variation of wave height and variation of heading angle, there was collision in the case whose dynamic amplitude factor was the highest among cases in which other variables are same. However, in Case 14, there was no collision. Fig. 11 shows the simulation results of Case 12 whose dynamic amplitude factor was the highest among cases in which there was collision.

3.2.4 Variation of wave period

Table 6 shows simulation results in which the wave height is 0.5 m, the wave period is varying 6.6 s to 10.4 s, the heading angle is 0˚, and the lifting off velocity is 0.1 m/s. There was collision only when the wave period is from 7.3 s to 8.9 s. The dynamic amplitude factor was the highest in Case 17. Fig. 12 shows the simulation results of Case 17. Fig. 12(a) shows the change of wire tension as time goes and Fig. 12(b) shows the moment of collision.

Table 4 Simulation results according to the variation of heading angle

Case	Wave height [m]	Wave period [s]	Heading angle [deg]	Lifting off velocity [m/s]	Maximum wire tension [ton]	Dynamic amplitude factor	Collision
5	0.4	11.4	0	0.1	1,050.950	1.051	X
6			45		1,066.112	1.066	X
7			90		1,076.763	1.077	O
8	0.6		0		1,073.185	1.073	X
9			45		1,081.989	1.082	O
10			90		1,091.462	**1.091**	O

Table 5 Simulation results according to the variation of lifting off velocity

Case	Wave height [m]	Wave period [s]	Heading angle [deg]	Lifting off velocity [m/s]	Maximum wire tension [ton]	Dynamic amplitude factor	Collision
11	0.2	11.4	45	0.04	1,039.732	1.040	O
12				0.05	1,046.006	1.046	O
13				0.06	1,045.274	1.045	X
14				0.07	1,048.724	**1.049**	X

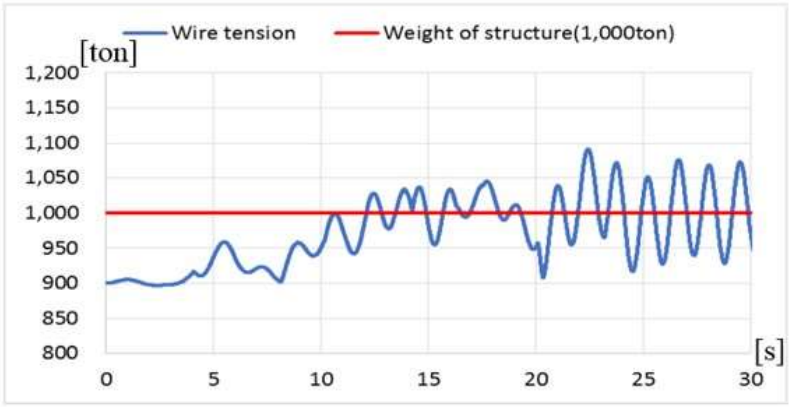

(a) Wire tension

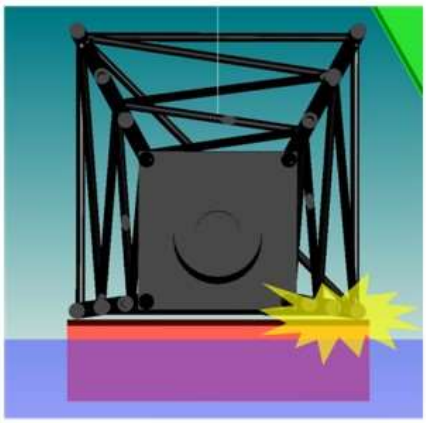

(b) Collision

Fig. 10 Simulation results of Case 10

(a) Wire tension

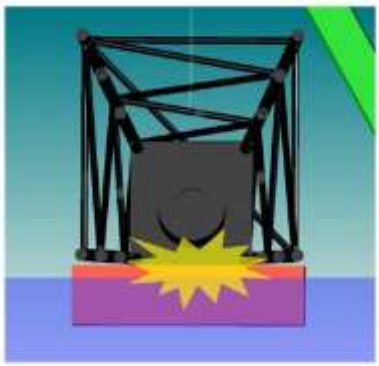

(b) Collision

Fig. 11 Simulation results of Case 12

Table 6 Simulation results according to the variation of wave period

Case	Wave height [m]	Wave period [s]	Heading angle [deg]	Lifting off velocity [m/s]	Maximum wire tension [ton]	Dynamic amplitude factor	Collision
15	0.5	10.4	0	0.1	1,055.415	1.055	X
16		9.6			1,065.626	1.066	X
17		8.9			1,107.652	**1.108**	O
18		8.3			1,106.704	1.107	O
19		7.8			1,089.457	1.089	O
20		7.3			1,096.011	1.096	O
21		6.9			1,081.213	1.081	X
22		6.6			1,091.178	1.091	X

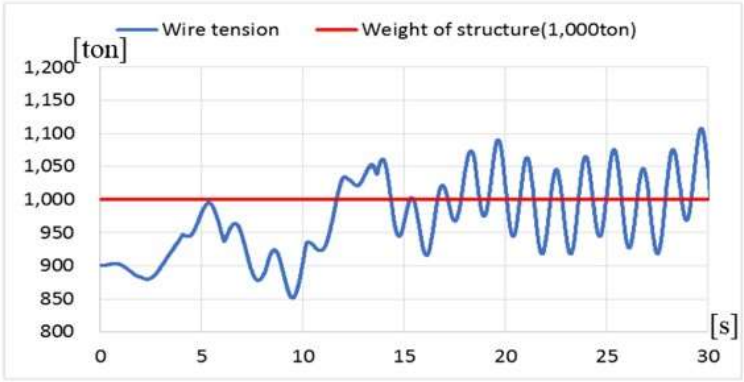

(a) Wire tension

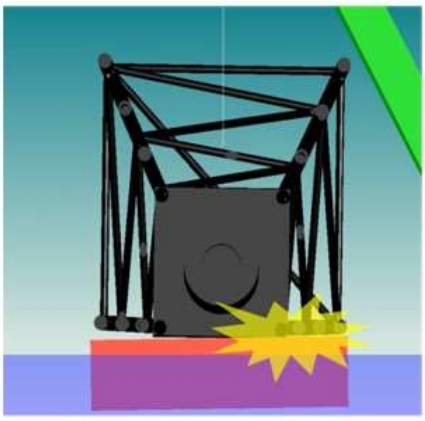

(b) Collision

Fig. 12 Simulation results of Case 17

3.2.5 Collision response of offshore structure

Fig. 13 shows the heave motion of the offshore structure in Cases 1, 4, 8, 10, 15, and 17. The conditions of Cases 1 and 4 are presented in Table 3. The conditions of Cases 8 and 10 are presented in Table 4. The conditions of Cases 15 and 17 are presented in Table 6. The lifting velocity of these cases are same as 0.1 m/s and the offshore structure is about to be lifted after about 15 s. There are horizontal intervals in the heave motion time series due to collision. Cases 4 (Fig. 13(b)), 10 (Fig. 13(d)), and 17 (Fig. 13(f)) in which collision occurred have horizontal intervals after about 15 s. These horizontal intervals are marked with red circles in Fig. 13. On the other hand, Cases 1 (Fig. 13(a)), 8 (Fig. 13(c)), and 15 (Fig. 13(e)) in which collision did not occur do not have horizontal intervals after about 15 s. These horizontal intervals reflect the collision response between the offshore structure and the transport barge.

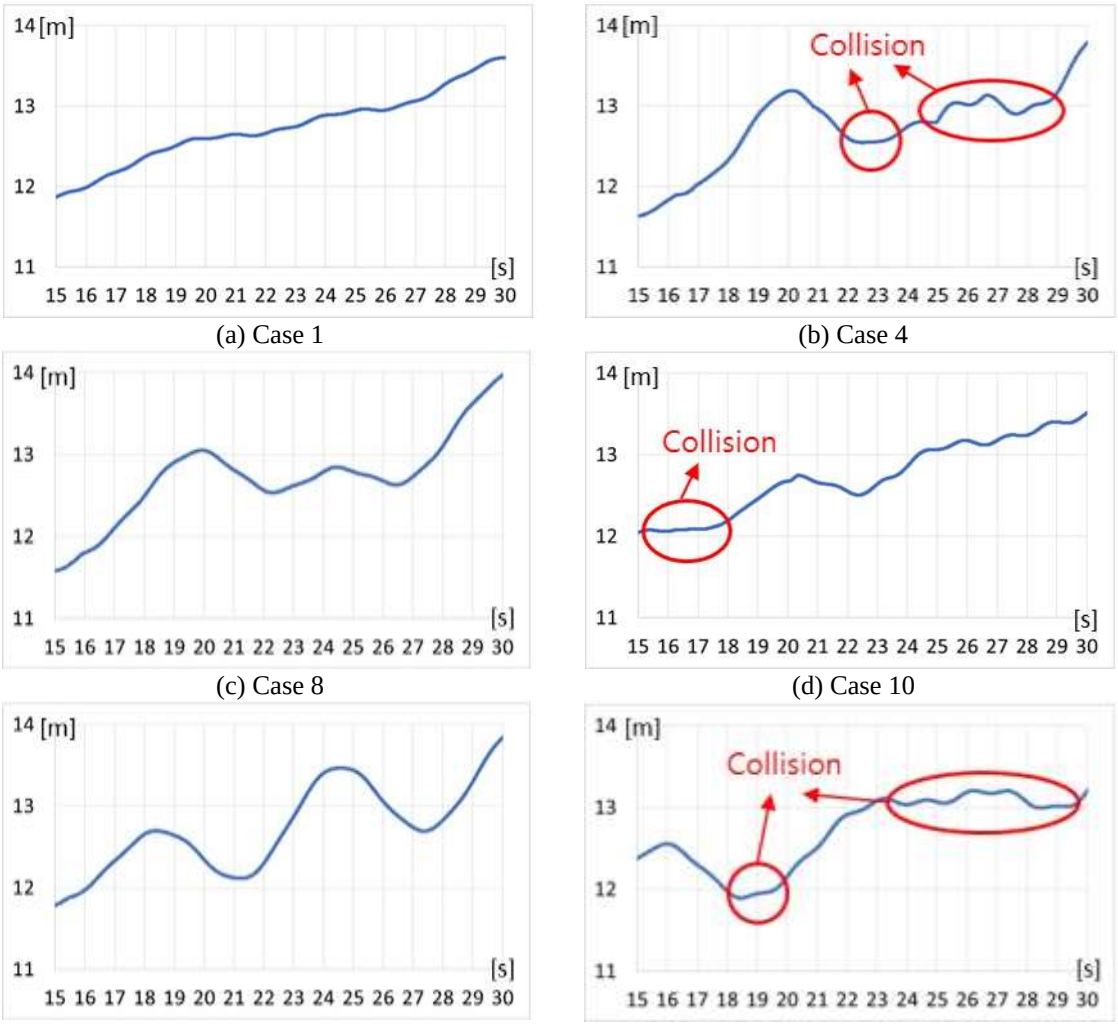

(a) Case 1 (b) Case 4

(c) Case 8 (d) Case 10

(e) Case 15 (f) Case 17

Fig. 13 The heave motion of the offshore structure of Cases 1, 4, 8, 10, 15, and 17

5. Conclusions

In this study, the physics-based simulation of the lifting off step while the OSV installs the structure was performed by varying operating conditions such as ocean environmental loads (wave height, heading angle, and wave period) and lifting off speed. The simulation is based on multibody system dynamics and collision process. For each operating condition, the tension acting on wire ropes of the OSV was calculated and the dynamic amplitude factor was determined from maximum tension. In addition, collision between the transport barge and the offshore structure was detected and the collision response of the offshore structure was checked by the heave motion of the offshore structure. For a certain operating condition, there was collision. From the simulation, the operability of the given operating condition could be investigated.

In the future, the way to quantify the sensitivity of the collisions to different ocean environmental loads will be studied. Also, dynamic positioning of the OSV, ocean environmental loads by irregular wave, and the interaction among floaters will be considered in the simulation. And, the simulation for other steps of the lifting operation such as lifting in the air, crossing splash zone, deeply submerging, and landing in Fig. 2 will be performed.

Acknowledgments

This work was partially supported by

a) BK21 Plus, Education & Research Center for Offshore Plant Engineers (COPE) of Seoul National University, Republic of Korea,

b) Engineering Research Institute of Seoul National University, Republic of Korea,

c) Research Institute of Marine Systems Engineering of Seoul National University, Republic of Korea, and

d) Engineering Development Research Center (EDRC) funded by the Ministry of Trade, Industry & Energy (MOTIE), Republic of Korea.

References

Boe, T. and Nestegard, A. (2010), "Dynamic forces during deepwater lifting operations", *Proceedings of the 10th International Offshore and Polar Engineering Conference*, Bejing, China, June

Cha, J.H., Roh, M.I. and Lee, K.Y. (2010a), "Integrated simulation framework for the process planning of ships and offshore structures", *Robot. Comput. -Integrated Manufacturing J.*, **26**(5), 430-453.

Cha, J.H., Roh, M.I. and Lee, K.Y. (2010b), "Dynamic response simulation of a heavy cargo suspended by a floating crane based on multibody system dynamics", *Ocean Eng*, **37**(14-15), 1273-1291.

Chris, H. (1997), *Collision Response*, Game Developer.

Cummins, W.E. (1962), "The impulse response function and ship motions", *Schiffstechnik*, **9**, 101-109.

Ha, S., Ku, N.K., Roh, M.I. and Hwang, H.J. (2015), "Multibody system dynamics simulator for process simulation of ships and offshore plants in shipyards", *Adv. Eng. Softw.*, **85**, 12-25.

Ku, N.K., Ha, S., Roh, M.I. and Lee, K.Y. (2013a), "Development of a kernel for dynamic analysis of various types of multi-crane in shipyard", *Proceedings of the 13th International Society of Offshore and Polar Engineers Computer Graphics*, Alaska, USA, June.

Ku, N.K., Cha, J.H., Roh, M.I. and Lee, K.Y. (2013b), "A tagline proportional-derivative control method for the anti-swing motion of a heavy load suspended by a floating crane in waves", *J. Eng. Maritime Environ.*, **227**(4), 357-366.

Ku, N.K. and Roh, M.I. (2014), "Dynamic response simulation of an offshore wind turbine suspended by a floating crane", accepted for publication in *Ships and Offshore Structures*, doi: 10.1080/17445302.2014.942504

Masoud, Z.N. (2000), *A control system for the reduction of cargo pendulation of ship-mounted cranes*, Ph.D. Dissertation, Virginia Polytechnic Institute and State University, Blacksburg.

Moore M. and Wilhelms J. (1988), "Collision detection and response for computer animation", *Comput. Graphics*, **22**(4), 289-298.

Nielsen, F.G. (2003), *Lecture Notes in Marine Operations*, Norwegian University of Science and Technology, Trondheim, Norway.

Shabana, A. (1994), *Computational Dynamics*, John Wieley & Sons, Inc.

Wu, M. (2013), *Dynamic analysis of a subsea module during splash-zone transit*, M.Sc. Dissertation, Norwegian University of Science and Technology, Trondheim.